

## SUPPLEMENTARY INFORMATION

### **The tectonic puzzle of the Messina area (Southern Italy): Insights from new seismic reflection data**

Carlo Doglioni<sup>1</sup>, Marco Ligi<sup>2</sup>, Davide Scrocca<sup>3</sup>, Sabina Bigi<sup>1,3</sup>, Giovanni Bortoluzzi<sup>2</sup>,  
Eugenio Carminati<sup>1</sup>, Marco Cuffaro<sup>3\*</sup>, Filippo D'Orlando<sup>2</sup>, Vittoria Forleo<sup>1</sup>, Filippo Muccini<sup>4</sup>,  
Federica Riguzzi<sup>5</sup>

<sup>1</sup>*Dipartimento di Scienze della Terra, Università Sapienza, P.le A. Moro 5, 00185 Roma, Italy.*

<sup>2</sup>*Istituto di Scienze Marine, CNR, U.O.S di Bologna, Via Gobetti 101, 40129 Bologna, Italy.*

<sup>3</sup>*Istituto di Geologia Ambientale e Geoingegneria, CNR, c/o Dipartimento di Scienze della Terra,  
Università Sapienza, P.le A. Moro 5, 00185 Roma, Italy.*

<sup>4</sup>*Istituto Nazionale di Geofisica e Vulcanologia, Roma2, Via Pezzino Basso 2, 19020, Fezzano (La  
Spezia), Italy.*

<sup>5</sup>*Istituto Nazionale di Geofisica e Vulcanologia, Roma, Via di Vigna Murata, 605, 00143 Roma, Italy.*

**This PDF file includes:  
Supplementary Figures (S1 to S11) and Table S1**

\*To whom correspondence should be addressed. E-mail: marco.cuffaro@igag.cnr.it

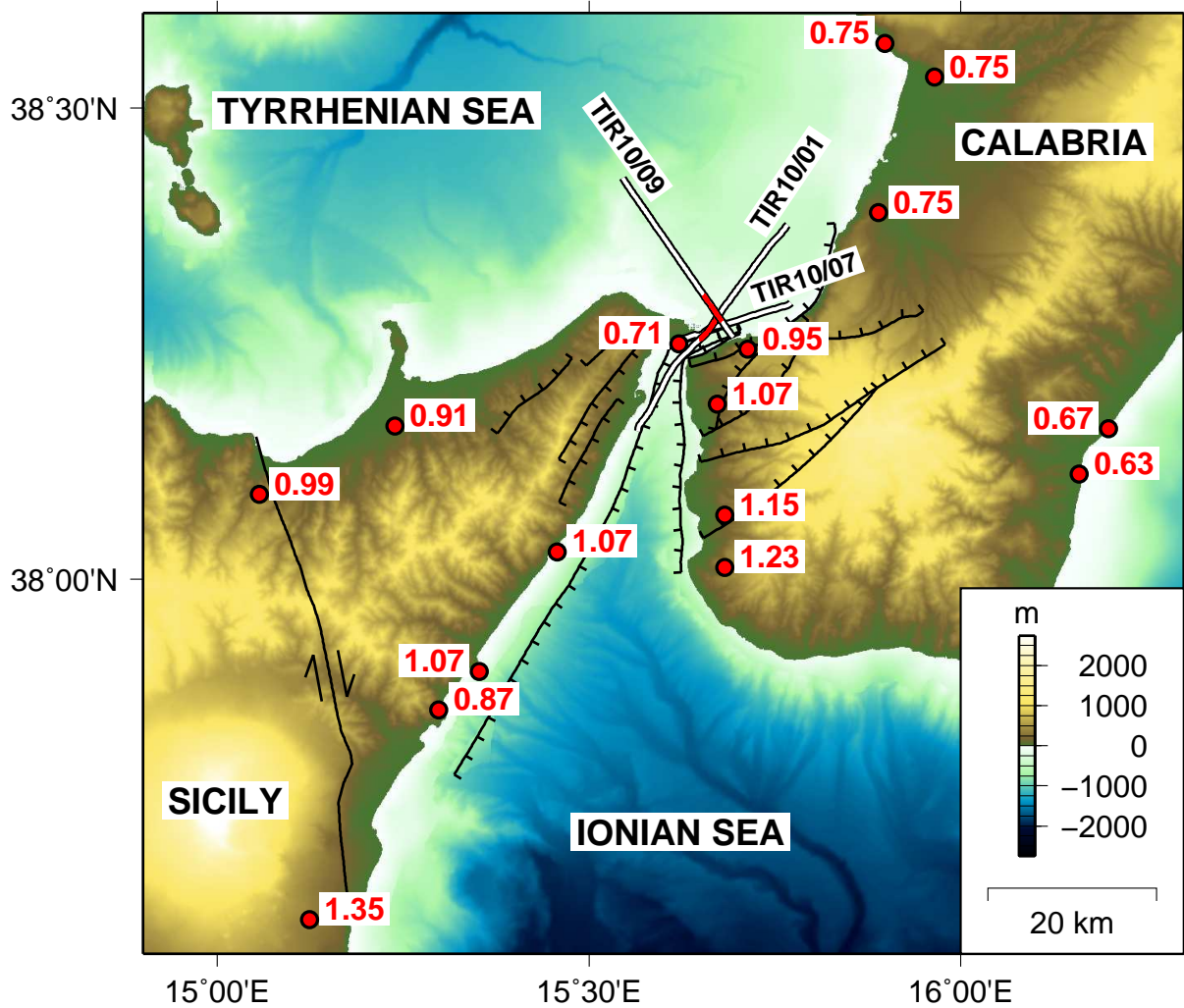


**Figure S1:** Topography of the study area and location of seismic profiles TIR10/01, TIR10/07, TIR10/09 (double black lines). Portions of profiles shown in Fig. S9 and Fig. S10 are highlighted by thick red lines. Red numbers indicate the average uplift rates of the area in mm/yr, based on the elevation of the MIS 5.5 (125 kyr) terraces from ref. 1.

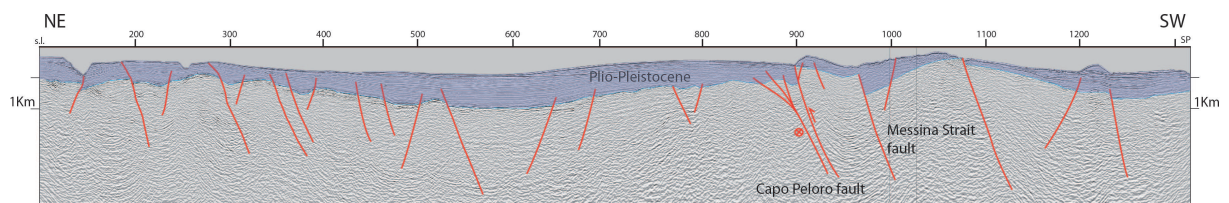


**Figure S2:** Depth converted seismic section TIR10/01. The conversion has been performed using the package Move2012 (Midland Valley) by the “polygons” procedure. See Table S1 for the parameters we used.

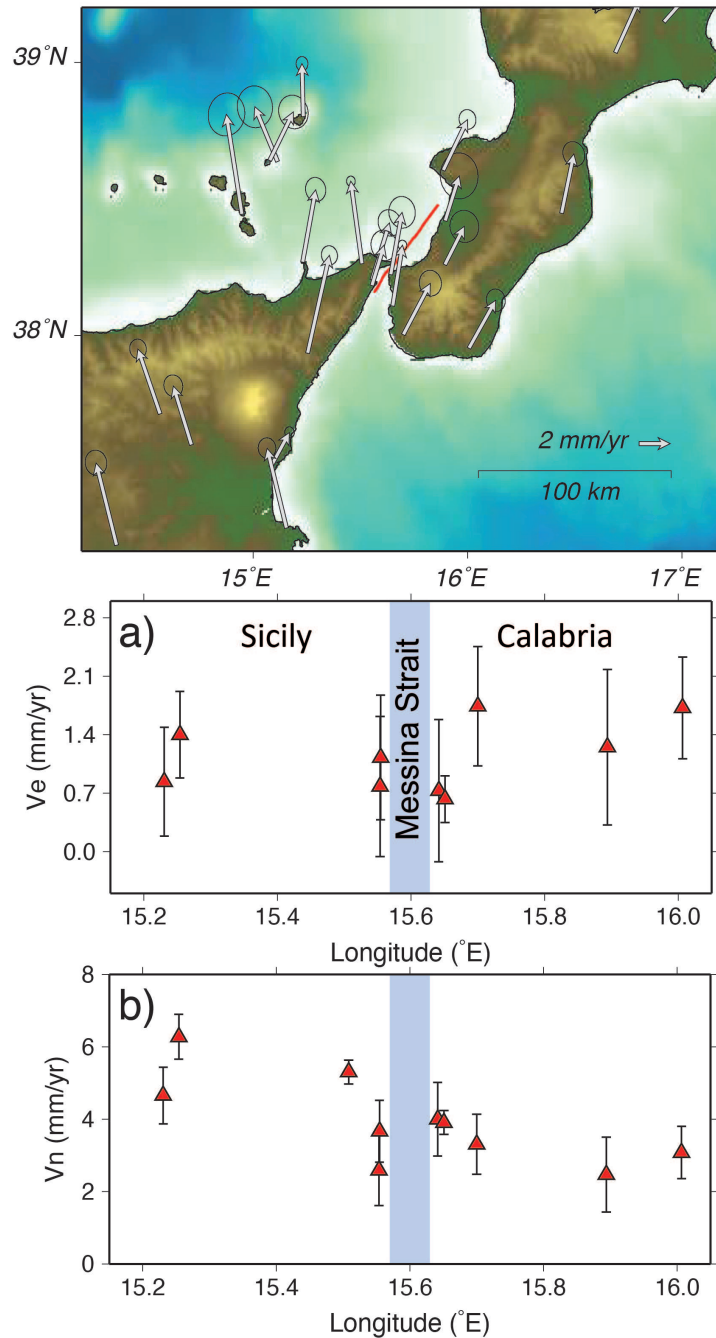


**Figure S3:** Horizontal GPS velocities relative to Eurasia and error ellipses representing the 68% confidence regions<sup>2</sup> (upper panel). The two cross-sections a) and b) show the projections of the velocity components ( $V_e$  and  $V_n$  respectively) along the W-E direction. On average, the Calabrian sites move eastward faster than the Sicilian sites (panel a), and Sicily is moving northward faster than Calabria (panel b). No significant motion is detected between the four sites strictly located across the Strait, if uncertainties are taken into account. The present velocity field indicates a right-lateral transtension in the area between Calabria and Sicily (e.g., along the Messina Strait). However, the Strait itself is presently not the seat where the maximum relative velocity between Calabria and Sicily is accommodated. The red line marks location of the seismic profile TIR10/01.

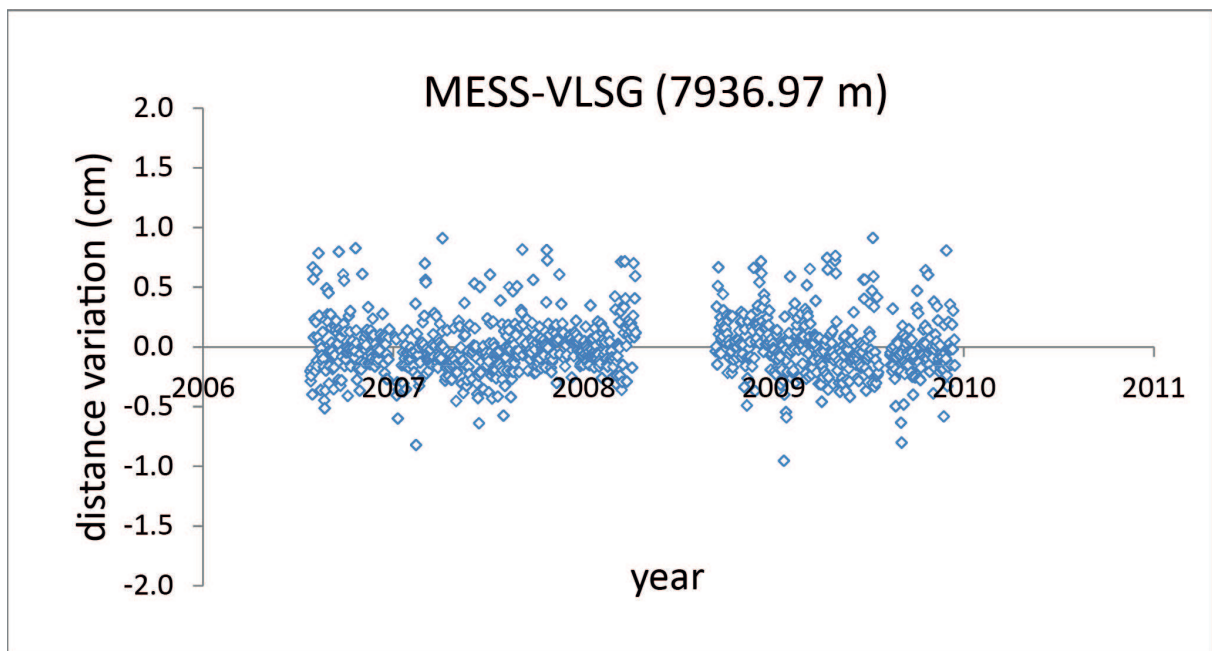


**Figure S4:** Cleaned time series of the 3D inter-distance variation between Messina (MESS) and Villa San Giovanni (VLSG) located just on the Strait opposite side. The mean inter-distance is 7936.97 m and its mean variation is  $0.00 \pm 0.24$  cm ( $1\sigma$  level). The significant extension rate detected in the area by some authors<sup>3</sup> is clearly not accommodated within the Strait. Extension is accommodated more inland Sicily, along the Tindari-Letojanni fault. The locked, lower strain rate, segment in the Messina Strait, indicates that the area is seismically loading, accumulating elastic energy.

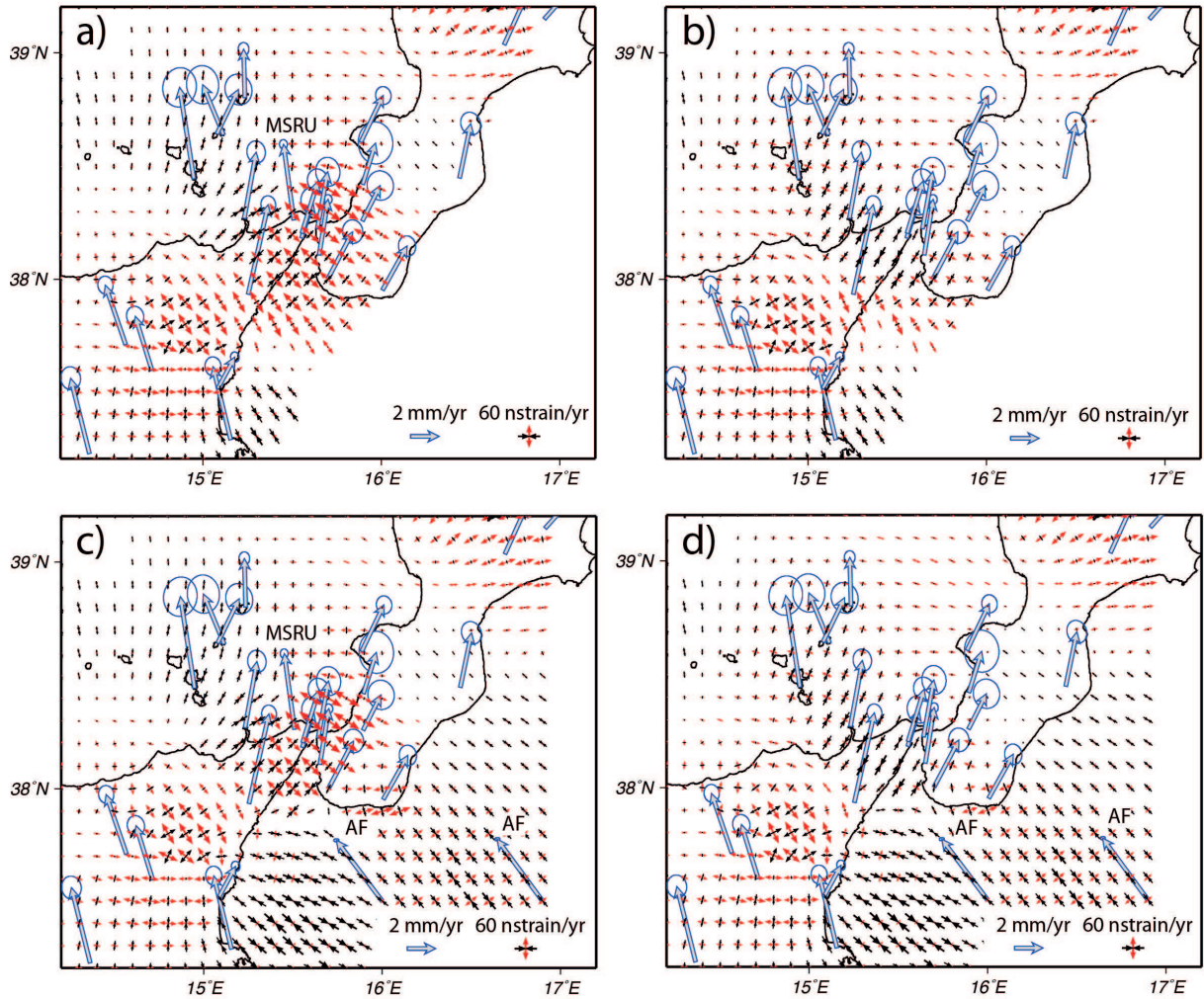


**Figure S5:** Principal axes of the 2D strain rate tensor computed over a regular grid ( $0.1^\circ \times 0.1^\circ$ ; red and black arrows are the extension and compression rates respectively). The Figure is composed by four panels just to show how complex is the data interpretation of the area: a) principal axes obtained from the whole GPS network; the extension appears as the prevailing tectonic style detected across the Strait, with value similar to those estimated by ref. 3; b) principal axes obtained after removing the velocity of MSRU; in this solution, to the north of the Strait the strain rates axes are almost equal and within the uncertainties, but moving southward, the dominant style becomes compressive ( $-58 \cdot 10^{-9} \text{ yr}^{-1}$ ) and directed along the strike of the Messina Strait. The last two panels show the previous two situations with the addition of two African velocities (computed from the pole and rotation rate of Africa<sup>4</sup>), in the hypothesis that the African push were transmitted unchanged to the Ionian area. Both panels c) and d) show a reinforced compressive component just south of the Strait.

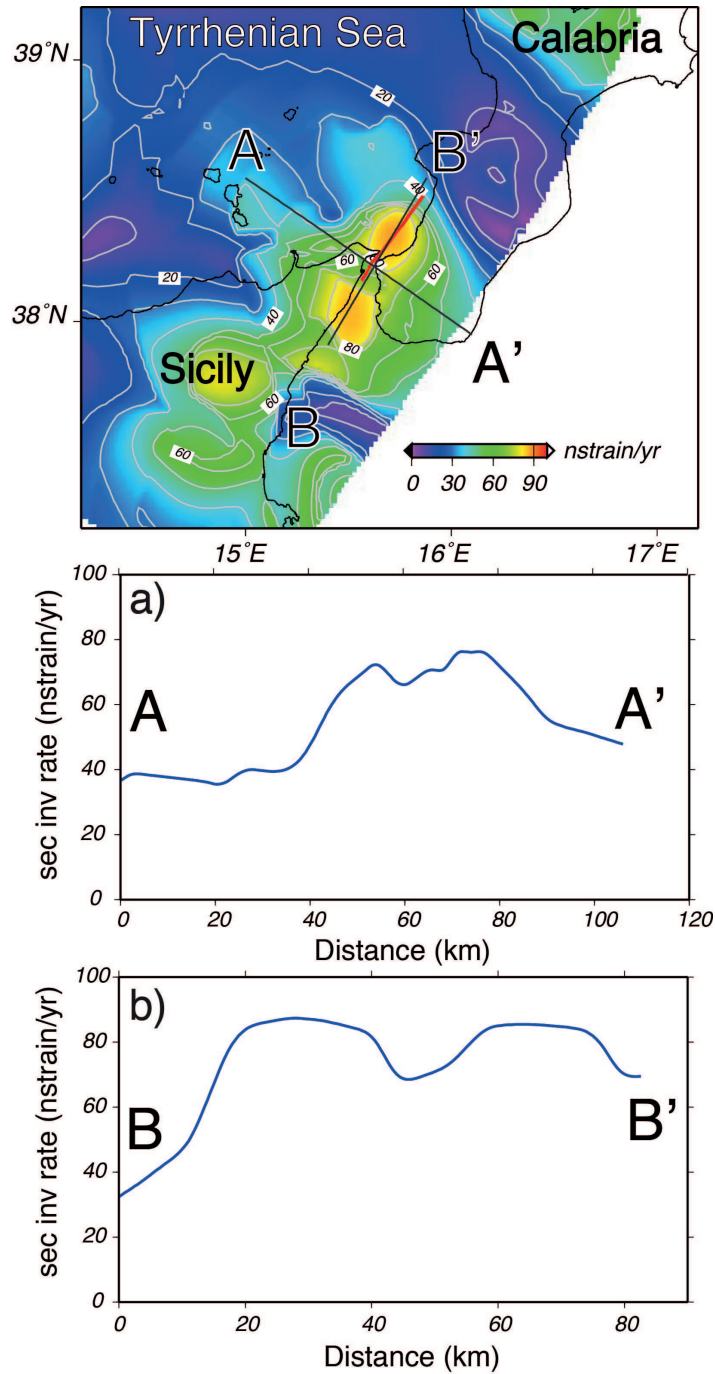


**Figure S6:** Map of the cumulative deformation rate (CDR), the second invariant of the 2D strain rate tensor (upper panel), and profiles a) and b) in the study area. The pattern of CDR is not uniform, reaching a maximum value of  $\approx 85 \cdot 10^{-9} \text{ yr}^{-1}$ ; note that in the central part of the Messina Strait, it decreases to a relative minimum of less than  $\approx 70 \cdot 10^{-9} \text{ yr}^{-1}$ . This indicates a more locked area where the tectonic loading is ongoing, a sector potential candidate near to next rupture. Red line: location of the seismic profile TIR10/01.

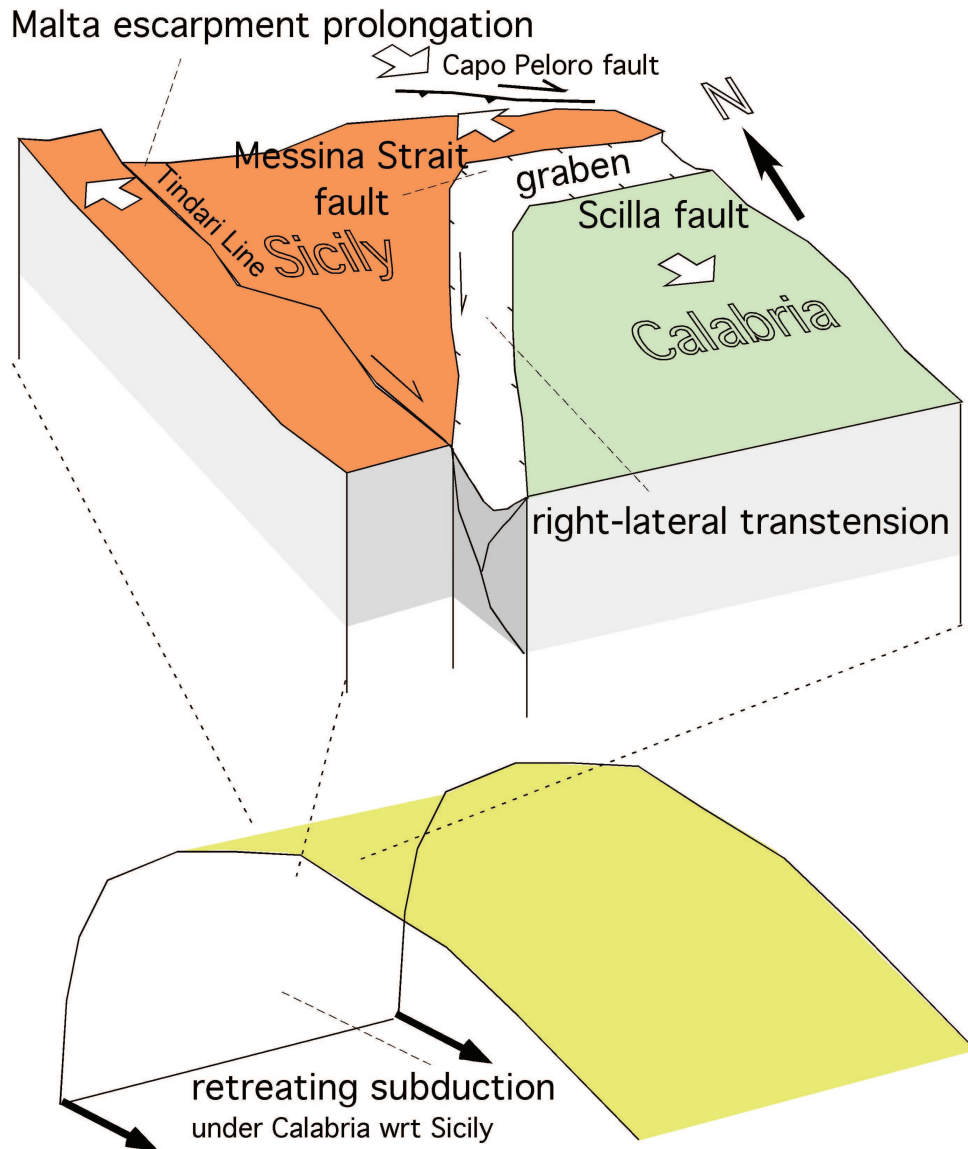
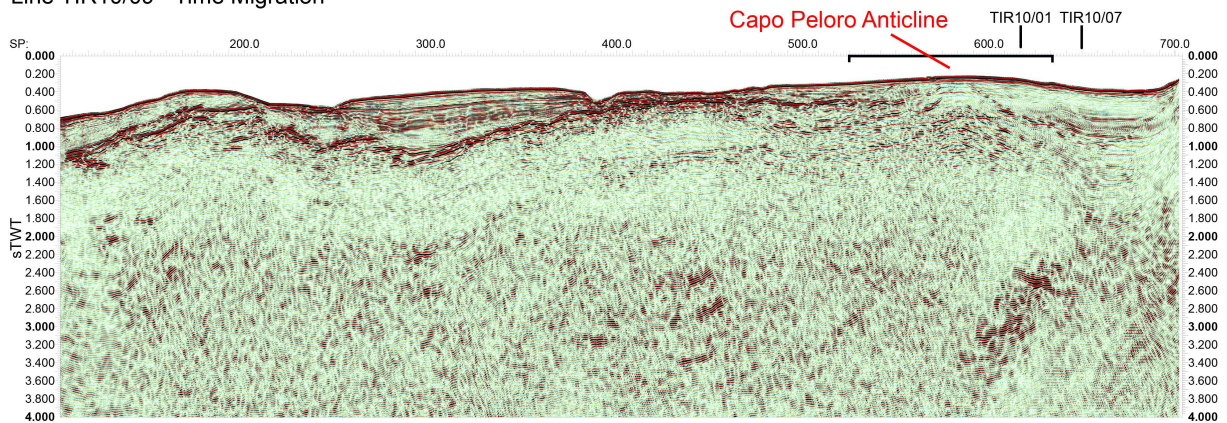


**Figure S7:** Sketch of the interpreted 3D tectonic setting. The Messina Strait is in the hangingwall of the Apennines-Calabrian subduction, and the extension in the area can be referred to the SE-ward retreat of the slab hinge. The Strait itself shows an undulate pattern of faults, depicting a graben in the northern part of the Strait, and a negative flower structure with right lateral transtension in the N-S trending segment. The northern Messina Strait appears as the seat of the transfer zone between the SSE-dipping Messina Strait normal fault shaping the main half graben visible in Fig. 3, and the NNW-dipping Scilla fault, which deeper part and related growth sedimentation are imaged in the seismic sections shown in Figs 4 and S8. Surface conjugate minor normal faults accompany this structural change on both sides of the basin. However, north of Capo Peloro, the area is rather undergoing right-lateral transpression.

Line TIR10/09 - Time Migration



Line TIR10/07 - Time Migration

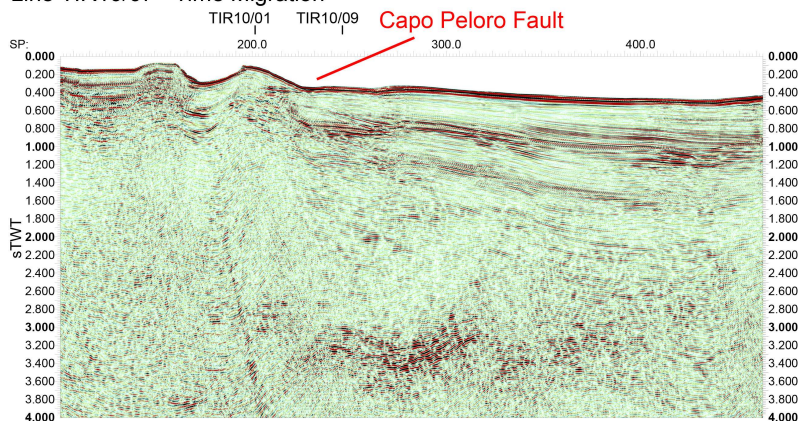


**Figure S8:** Time migrated seismic reflection profile TIR10/09 (upper panel) and TIR10/07 (lower panel). The location of the two sections is in Fig. S1. Note the position of the Capo Peloro Anticline and the Capo Peloro Fault in the two profiles respectively, and the locations of the intersections with the other seismic profiles used in this study. The Scilla fault is visible in the lower right side of TIR10/09, and the related growth sedimentation in the right side of TIR10/07. This last profile strikes almost parallel to the Messina Strait and Scilla faults, showing the asymmetry of the transfer zone among the two related half grabens. The black line on top of the upper panel marks the portion of profile TIR10/09 shown in Fig. 5.



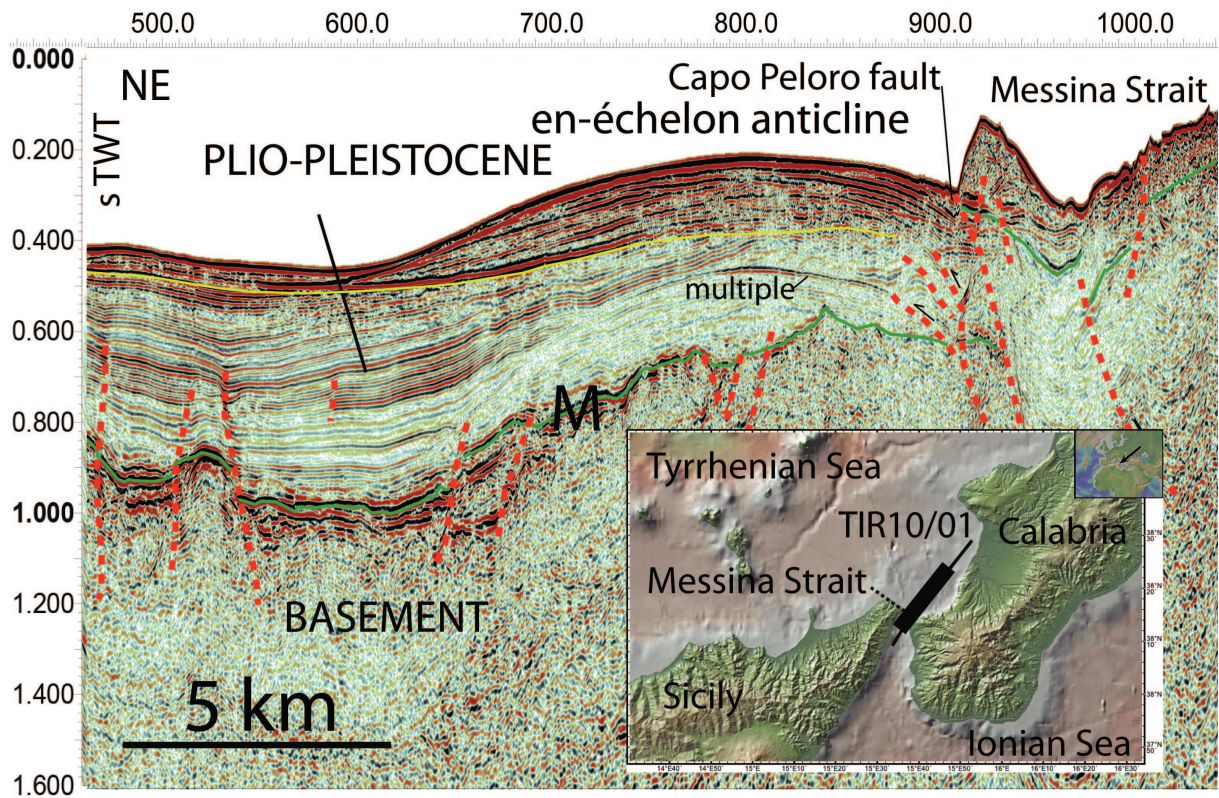


**Figure S9:** Close-up of the seismic reflection profile TIR10/01, showing in more detail the marked unconformities of Fig. 3. M, Messinian unconformity, green line. In yellow the intra-Plio-Pleistocene unconformity. Note the syncline-anticline pair involving both the sedimentary cover and the underlying “basement”, as well as the Capo Peloro fault to the southwest.

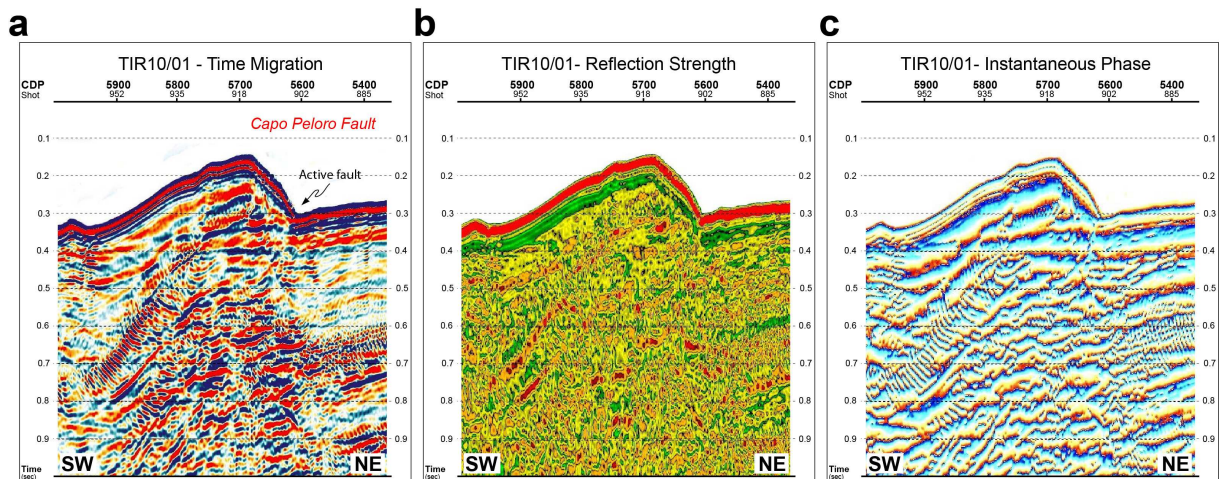


**Figure S10:** Close-up and instantaneous attributes of portion of the seismic reflection profile TIR10/01 in Fig. 3, showing structural details and recent activity of the Capo Peloro fault. Note the fault scarp in the sea-floor, and the subvertical attitude of the fault separating rocks of different acoustic amplitude when comparing the two walls.

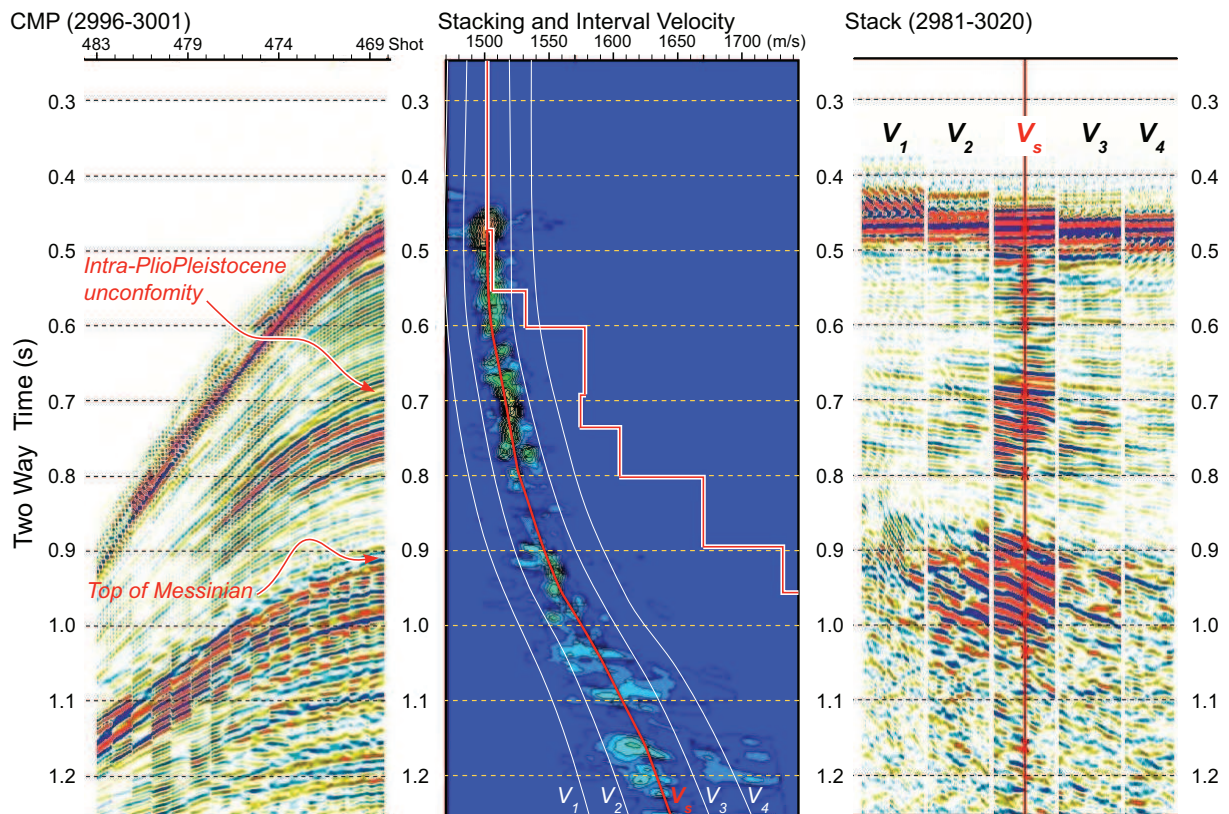


**Figure S11:** Example of Velocity analysis along line TIR10/01. **Left:** CMP supergather (6 CMPs); **centre:** stacking velocity picking and Dix's interval velocity; **right:** stacked panels obtained by adopting the picked stacking velocity function ( $V_s$ ) and velocity functions with lower and higher values than stacking velocities.

**Table S1:** Published interval velocities adopted for the depth conversion of the Plio-Pleistocene units in the Sicilian offshore areas around the Messina Straits<sup>5-7</sup>.

Units (Ages)	Velocity (m/s)		
	ODP (Ref. <sup>5</sup> )	Ref. <sup>6</sup>	Ref. <sup>7</sup>
Pleistocene– Middle Pliocene	1700	1800	2000
Lower Pliocene		1900	

## References

- [1] Antonioli, F. *et al.* Late Pleistocene to Holocene record of changing uplift-rates in southern Calabria and northeastern Sicily (southern Italy, Central Mediterranean Sea). *Tectonophysics* **422**, 23–40 (2006).
- [2] Devoti, R., Esposito, A., Pietrantonio, G., Pisani, A. R. & Riguzzi, F. Evidence of large scale deformation patterns from GPS data in the Italian subduction boundary. *Earth Planet. Sci. Lett.* **331**, 230–241 (2011).
- [3] Serpelloni, E. *et al.* Strain accumulation across the Messina Straits and kinematics of Sicily and Calabria from GPS data and dislocation modeling. *Earth Planet. Sci. Lett.* **298**, 347–360 (2010).
- [4] Altamimi, Z., Collilieux, X., Legrand, J., Garayt, B. & Boucher, C. ITRF2005: A new release of the International Terrestrial Reference Frame based on time series of station positions and Earth Orientation Parameters. *J. Geophys. Res.* **112** (2007).
- [5] Mascle, J. & Rehault, J. P. A revised seismic stratigraphy of the Tyrrhenian Sea: implications for the basin evolution. In Kastens, K. A., Mascle, J. & et al. (eds.) *Proceedings of the Ocean Drilling Program, Scientific Results*, vol. 107, 617–636 (1990).
- [6] Pepe, F., Bertotti, G., Cella, F. & Marsella, E. Rifted margin formation in the south Tyrrhenian Sea: a high-resolution seismic profile across the north Sicily passive continental margin. *Tectonics* **19**, 241–257 (2000).
- [7] Catalano, R., Franchino, A., Merlini, S. & Sulli, A. Central western Sicily structural setting interpreted from seismic reflection profiles. *Mem. Soc. Geol. It.* **55**, 5–16 (2000).